Orientation of trimethylolethane cyclic phosphite in rhodium complexes: structure of [Rh($CH_3COCHCOCH_3$)(CO)($P(OCH_2)_3CCH_3$)]

Petrus H.van Rooyen,[b] Jeanet Conradie[a,*]

[a] Department of Chemistry, PO Box 339, University of the Free State, 9300 Bloemfontein, Republic of South Africa.

[b] Department of Chemistry, University of Pretoria, Private Bag X20, Hatfield, 0028, South Africa.

*Contact author details:

Name: Jeanet Conradie

Tel: +27-51-4012194

Fax: +27-51-44017295

e-mail: conradj@ufs.ac.za

Keywords

Rhodium; β-Diketone; Structure; DFT; Cyclic phosphite

Graphical abstract

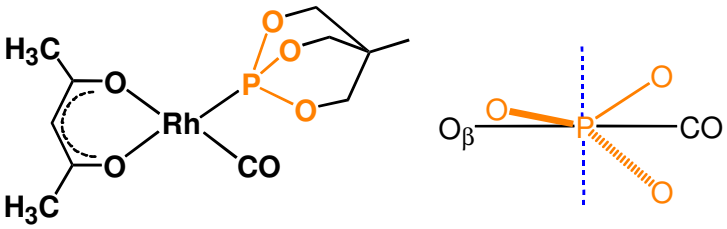

Synopsis

$P(OCH_2)_3CCH_3$ rotation and orientation in [Rh($CH_3COCHCOCH_3$)(CO)($P(OCH_2)_3CCH_3$)].

Highlights

$P(OCH_2)_3CCH_3$ containing Rh complexes

$P(OCH_2)_3CCH_3$ rotation and orientation

Crystal structure of $[Rh(CH_3COCHCOCH_3)(CO)(P(OCH_2)_3CCH_3)]$ (**1**)

Conformational preference of $P(OCH_2)_3CCH_3$ in (**1**)

Abstract

Density functional theory calculations showed that rotation of the ($P(OCH_2)_3CCH_3$) group in the rhodium-acetylacetonato complex $[Rh(acac)(CO)(P(OCH_2)_3CCH_3)]$ has a negligible influence on the energy of the complex. Density functional theory calculations further showed that the minimum energy orientation of the cyclic ($P(OCH_2)_3CCH_3$) group in square planar rhodium-($P(OCH_2)_3CCH_3$)-(CO) complexes containing a bidentate ligand that is larger than the acetylacetonato ligand, is with one of the P-O bonds near parallel (within 10°) to the plane defined by the four atoms coordinated to Rh. The three P-O bonds of the rigid ($P(OCH_2)_3CCH_3$) group adopt a C_3-symmetrical conformation around the Rh-P axis. The lowest energy geometry of $[Rh(BID)(CO)(P(OCH_2)_3CCH_3)]$ (BID = bidentate ligand with two O donor atoms and charge -1) complexes is where one P-O bond is aligned near parallel to the $Rh\text{-}O_{BID\ \textit{trans to}\ CO}$ bond, while the geometry with a P-O bond orientated near parallel to the $Rh\text{-}C_{CO}$ bond, is slightly higher in energy, but still possible experimentally. The highest energy orientation of the ($P(OCH_2)_3CCH_3$) group in square planar $[Rh(BID)(CO)(P(OCH_2)_3CCH_3)]$ complexes, is with one of the P-O bonds near perpendicular to the plane described by the four atoms coordinated to Rh. The orientation of the cyclic ($P(OCH_2)_3CCH_3$) group in available experimental structures of square planar [Rh(BID)(CO) ($P(OCH_2)_3CCH_3$)] complexes, confirms this finding.

1 Introduction

Rhodium complexes are often used as catalysts in industrial processes. Probably the most well-known and most cited industrial process using a rhodium catalyst, is the Monsanto process of manufacturing acetic acid by the catalytic carbonylation of methanol [1]. The global acetic acid market is very important, since it is a precursor for the manufacturing of various other chemicals (e.g. monochloroacetic acid, camphor, diketene and photographic chemicals) that are intermediates for various end user industries, such as textiles, inks, coatings, rubbers, greases, plastics, adhesives, sealants and others. The global acetic acid market was valued at more than 14 000 Kilotons in 2014

[2,3]. The original acetic acid manufacturing process was developed in 1960 by the German chemical company BASF. During this process acetic acid is formed from methanol and carbon monoxide, with co-catalysts of cobalt and iodide, at conditions of 300 ºC and 700 atmosphere. In 1966 the Monsanto Company improved the experimental conditions by using a new catalyst system of rhodium/iodide ion co-catalysts that operate at milder conditions of 150 - 200 ºC and 30 - 60 atmosphere. The Monsanto Company commercialised this process in 1970. Currently, the acetic acid manufacturing process has largely been substituted by the Cativa process which uses a similar, though more economical and environmentally friendly, iridium-based process, developed by BP Chemicals Ltd [4,5]. However, the former harsh conditions of the manufacturing process still spurred researchers on to search for new catalysts which work under milder conditions. The design of catalysts specifically focused on designing ligands which would increase the electron density at the metal, in order to promote oxidative addition reaction of methyl iodide to the catalyst, which is the rate-determining step of the rhodium-based catalytic cycle. One class of ligands which proved to be highly active carbonylation catalysts when coordinated to Rh(I) complexes, are phosphorous-containing ligands, due to their good σ-donor properties and their π-capability [6]. For example, trialkylphosphines-rhodium complexes leads to a more electron-rich rhodium centre such as the catalyst precursor $[Rh(PEt_3)_2(CO)Cl]$ that catalyses the carbonylation of methanol to form acetic acid at a rate nearly twice as high as that of $[Rh(CO)_2I_2]^-$ [7,8]. β-diketonato ligands containing electron donating substituents, as well as tertiary phosphines and phosphites, proved to increase the rate of oxidative addition of methyl iodide to complexes of the type [Rh(β-diketonato)(CO)(PPh_3)] [9,10,11,12], [Rh(β-diketonato)($P(OPh)_3)_2$] [13,14,15] and also [Rh(β-diketonato)(CO)($P(OCH_2)_3CCH_3$)] [16,17,18]. The rhodium-β-diketonato-phosphite complex [Rh(acac)(CO)($P(OCH_2)_3CCH_3$)], oxidatively adds methyl iodide *ca* 300 times faster than the Monsanto catalyst, while the next step in the catalytic cycle, the carbonyl insertion step, is of the same order than the rate-determining oxidative addition step of iodomethane to $[Rh(CO)_2I_2]^-$ [19]. The optimization of the catalytic activity of a catalyst often focuses on modifications of the primary coordination sphere of the metal, by improving the electronic and steric properties of the ligands that are coordinated to the metal centre [20]. An understanding of the conformational preferences of tertiary phosphine-containing complexes is important for the development of improved catalysts. We previously reported on the conformational preferences of triphenylphosphine in square planar organometallic complexes [21], as well as on the conformational preferences of the PR_3 groups diphenyl-2-pyridylphoshine and triphenylphosphine in square planar [Rh(β-diketonato)(CO)(PR_3)] complexes [22,23,24]. We were interested to determine whether the trimethylolethane cyclic phosphite group also exhibits a conformational preference when coordinated to square planar rhodium complexes.

In this contribution we thus present a combined density functional and solid state crystal structure study of the β-diketonato- as well as phosphite-containing complex [Rh(acac)(CO)(P(OCH$_2$)$_3$CCH$_3$)], (**1**), (Hacac = CH$_3$COCH$_2$COCH$_3$ = acetylacetone). Special focus will be given on the orientation of the tertiary phosphite group in complex (**1**) and related rhodium complexes that also contain a bidentate ligand, namely dbm (dibenzoylmethanato) in complex (**2**) [25], or cupf (N-aryl-N-nitrosohydroxylaminato) in complexes (**3**) [26] and (**4**) [27], see **Scheme 1**.

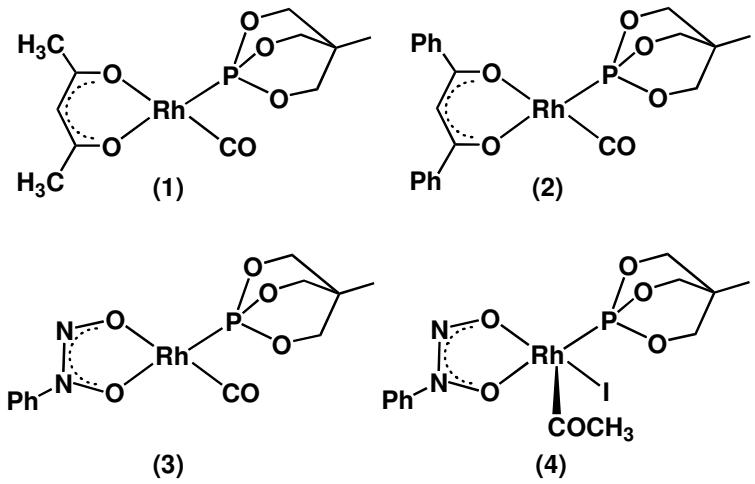

Scheme 1: The phosphite-containing rhodium complexes of this study: [Rh^{I}(acac)(CO)(P(OCH$_2$)$_3$CCH$_3$)] (**1**), [Rh^{I}(dbm)(CO)(P(OCH$_2$)$_3$CCH$_3$)] (Hdbm = dibenzoylmethane) (**2**) [25], [Rh^{I}(cupf)(CO)(P(OCH$_2$)$_3$CCH$_3$)] (cupf = N-aryl-N-nitrosohydroxylaminato) (**3**) [26] and [Rh^{III}(cupf)(COCH$_3$)(I))(P(OCH$_2$)$_3$CCH$_3$)] (**4**) [27].

2 Experimental

2.1 Synthesis

[Rh(acac)(CO)(P(OCH$_2$)$_3$CCH$_3$)] (**1**),was synthesized as described previously [19], from [Rh(acac)(CO)$_2$] (dicarbonyl(acetylacetonato)-rhodium(I)) [28], and P(OCH$_2$)$_3$CCH$_3$, (4-methyl-2,6,7-trioxa-1-phosphabicyclo[2.2.2]octane or trimethylolethane cyclic phosphite) [29].

2.2 Crystal structure analysis

Data for the crystals, obtained from solutions in hexane, were collected on a Bruker D8 Venture kappa geometry diffractometer, with duo Iμs sources, a Photon 100 CMOS detector and APEX II [30] control software, using Quazar multi-layer optics monochromated, Mo-*K*α radiation

by means of a combination of ϕ and ω scans. Data reduction was performed, using SAINT+ [30] and the intensities were corrected for absorption, using SADABS [30]. The structure was solved by intrinsic phasing, using SHELXTS and refined by full-matrix least squares, using SHELXTL + [31] and SHELXL-2013+ [31]. In the structure refinement, all hydrogen atoms were included in experimental positions determined from successive electron difference maps, and refined without any restrictions but with a common isotropic thermal parameter. All non-hydrogen atoms were refined with anisotropic displacement parameters. Crystal data and structural refinement parameters are given in the electronic supplementary information.

2.3 Density functional theory (DFT) calculations

Density functional theory (DFT) calculations were carried out, using the ADF (Amsterdam Density Functional) 2013 programme [32] with the PW91 (Perdew-Wang 1991) [33] GGA (Generalized Gradient Approximation) functional. The TZP (Triple ζ polarized) basis set, with a fine mesh for numerical integration and full geometry optimization, applying tight convergence criteria, was used for minimum energy searches.

3 Results and Discussion

3.1 X-ray structure

Perspective drawings [34] of the molecular structure of one of the two molecules of [Rh(acac)(CO)(P(OCH_2)$_3$$CCH_3$)], (**1**), in the asymmetric unit, showing the crystallographic numbering scheme used, are presented in Figure 1. Table 2 gives selected geometrical parameters of [Rh(acac)(CO)(P(OCH_2)$_3$$CCH_3$)], (**1**), and related Rh-(P(OCH_2)$_3$$CCH_3$) complexes (**2**) [25], (**3**) [26] and (**4**) [27]. A summary of some of the important crystal data is as follows: Empirical formula: C_{11} H_{16} O_6 P Rh; monoclinic space group: C 2/c; unit cell dimensions: a = 30.358(16), b = 14.838(7) , c = 13.156(6) Å, β = 105.01(2)°; volume = 5724(5) Å^3; Z = 16; crystal size = 0.325 x 0.223 x 0.101 mm^3; theta range for data collection 2.348 to 28.315°; independent reflections = 7106 [R(int) = 0.0442]; completeness to theta = 25.242° = 99.9 %; data / restraints / parameters = 7106 / 0 / 440; goodness-of-fit on F^2 = 1.062; final R indices [I>2sigma(I)] : R1 = 0.0180, wR2 = 0.0396; R indices (all data): R1 = 0.0229, wR2 = 0.0411; largest diff. peak and hole = 0.380 and -0.497 e.Å^{-3}. The complete crystal data and structure refinement details of (**1**) are given in the Supporting Information.

There are four weak intermolecular hydrogen bonds observed in the crystallographic packing of (**1**) (see data in Table 1): O1---H2B, O2---H31A, O3---H23A and O25---H9B at distances varying between 2.60(2) and 2.63(2) Å respectively. However, the A---H—D angle for O1---H2B—C2 at 113.0(15) is significantly more non-linear than the other contact angles that vary between 144.7(17) and 155.3(18), suggesting that the latter three contacts are mainly responsible for the packing in the solid state.

Table 1: Hydrogen bonds observed in the crystallographic packing of [Rh(acac)(CO)(P(OCH_2)$_3$$CCH_3$)] (**1**):

Atoms A---H—D	Distance A---H / Å	Angle / ° A---H—D
O1---H2B—C2	2.62(2)	113.0(15)
O2---H31A—C31	2.60(2)	152.1 (18)
O3---H23A—C23	2.63(2)	144.7(17)
O25---H9B—C9	2.60(2)	155.3(18)

In addition, there are two H-atoms interacting in a perpendicular orientation with the π sytems in the acac units: the C-H…ring centroid distances observed for H29A---ring1 (Rh1-O4-C5-C6-O5) and H29B---ring2 (Rh21-O24-C25-C26-O25) are 2.60(2) and 2.63 (2) Å, respectively. See Figure S1 in the Supporting Information for a packing diagram of (**1**).

The dihedral angle O_{acac} *trans* to CO-Rh-P-O, reflects the orientation of the trimethylolethane cyclic phosphite group (P(OCH_2)$_3$$CCH_3$). As such, the O4-Rh1-P1-O3 and O23-Rh21-P21-O23 dihedral angles of the two molecules in the asymmetric unit of (**1**), are very similar, namely -24.32(7)° and -33.19(7)°, respectively; see Figure 2.

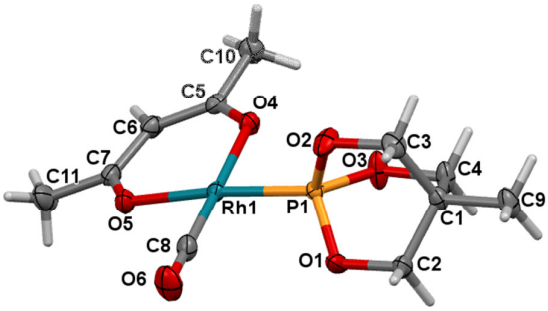

Figure 1: A perspective drawing of the molecular structure of one of the two molecules in the asymmetric unit of [Rh(acac)(CO)(P(OCH$_2$)$_3$CCH$_3$)] (**1**), showing the atom numbering scheme. Atomic displacement parameters (ADPs) are shown at the 50 % probability level.

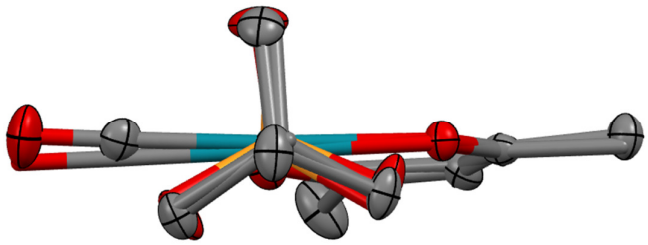

Figure 2: A perspective view of the orientation of the overlapped two molecules of [Rh(acac)(CO)(P(OCH$_2$)$_3$CCH$_3$)] (**1**), viewed along the P-Rh bond. Hydrogen atoms were omitted for clarity.

Table 2: Selected geometric parameters for [Rh(acac)(CO)($P(OCH_2)_3CCH_3$)] (**1**) and related [Rh(BID)(CO)($P(OCH_2)_3CCH_3$)] (BID = bidentate ligand with two O donor atoms and charge -1) complexes.

Complex	Distance in Å				Dihedral angle $O_{BID\ trans\ to\ CO/I}$-Rh-P-O	CCDC code	Reference
	Rh-P	Rh-C_{CO} or Rh-C_{acyl}	Rh-O (*trans* P or I)	Rh-O (*trans* CO)			
[Rh(acac)(CO)($P(OCH_2)_3CCH_3$)], (**1**),molecule 1	2.178	1.829	2.069	2.045	-24.32(7)	this study	this study
[Rh(acac)(CO)($P(OCH_2)_3CCH_3$)], (**1**), molecule 2	2.178	1.830	2.069	2.050	-33.19(7)	this study	this study
[Rh(dbm)(CO)($P(OCH_2)_3CCH_3$)], (**2**)	2.169	1.803	2.060	2.031	-10.7(2)	NUTKOC	25
[Rh(cupf)(CO)($P(OCH_2)_3CCH_3$)], (**3**)	2.156	1.772	2.026	2.059	-179.3(3)	TANLUP	26
[Rh(cupf)($COCH_3$)(I))($P(OCH_2)_3CCH_3$)], (**4**)	2.186	2.039	2.043	2.053	-34.7(3); +34.7(3)	DUJZOY	27

3.2 Computational chemistry study

To evaluate the preferred minimum energy orientation of the trimethylolethane cyclic phosphite group ($P(OCH_2)_3CCH_3$) in complexes (**1**)-(**4**), a potential energy scan (PES) of the rotation of ($P(OCH_2)_3CCH_3$) around the Rh-P bond in each of the complexes (**1**)-(**4**) was determined; see **Figure 3**. The three P-O bonds of the rigid ($P(OCH_2)_3CCH_3$) group adopt a C_3-symmetrical conformation around the Rh-P axis and therefore the PES scan is repeated after a rotation of 120°. From the PES it is clear that rotation of the cyclic ($P(OCH_2)_3CCH_3$) group has a negligible influence on the energy of square-planar complex (**1**), since the difference between the maximum and minimum energy during the PES for (**1**) is only 0.005 eV. This small energy difference implies that the ($P(OCH_2)_3CCH_3$) group could virtually adopt any orientation in (**1**), including the two slightly different orientations of the ($P(OCH_2)_3CCH_3$) group in the experimental structure of molecule 1 and molecule 2 of complex (**1**); see **Figure 4** (a). The orientation of the ($P(OCH_2)_3CCH_3$) group in the optimized geometries (using strict convergence parameters) of the maximum and minimum energy orientations of the ($P(OCH_2)_3CCH_3$) group in complex (**1**), with a negligible energy difference of 0.001 eV, is illustrated in **Figure 4** (b). The minimum energy orientation of the ($P(OCH_2)_3CCH_3$) group in complex (**1**) can be described by one of the P-O bonds near parallel to the plane (orientation 1 with dihedral angle $O_{acac\ \textit{trans to CO}}$-Rh-P-O ≈ 5°, should be 0° for exactly parallel) through the four atoms coordinated to Rh. The high energy orientation is when one of the P-O bonds is near perpendicular to the plane through the four atoms coordinated to Rh (orientation 2 with the three dihedral angles $O_{acac\ \textit{trans to CO}}$-Rh-P-O ≈ 34°, 85° and 155°, should be 45°, 90° and 135°, respectively, for exactly perpendicular), as shown in in **Figure 4** (b) and illustrated in **Scheme 2**.

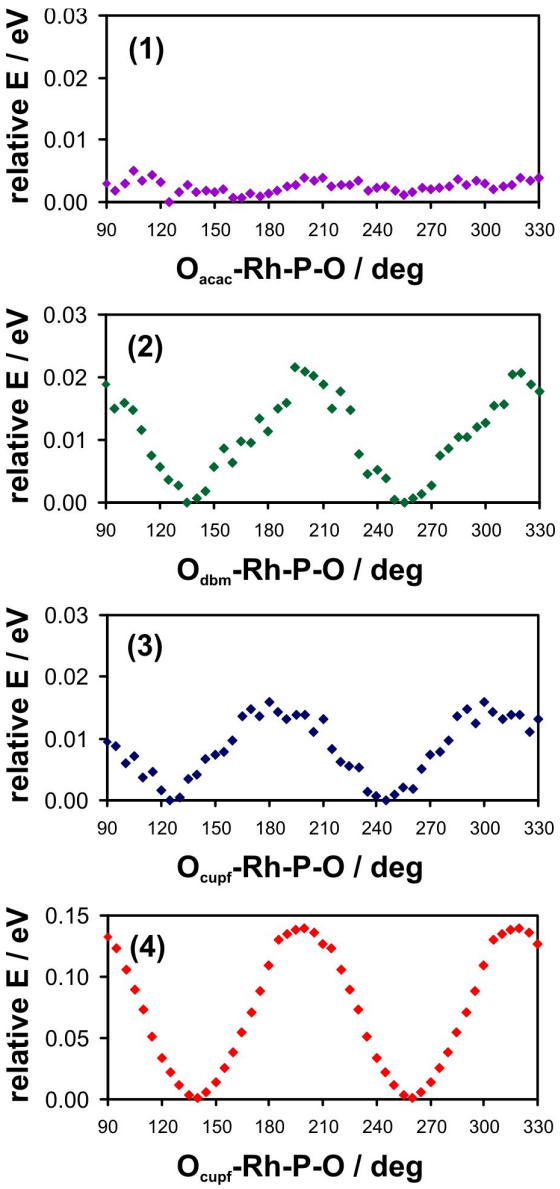

Figure 3: PES of the rotation of the cyclic ($P(OCH_2)_3CCH_3$) group around the Rh-P bond (as a function of the dihedral angle, O_{BID} *trans* to CO/I-Rh-P-O) in complexes (**1**)-(**4**).

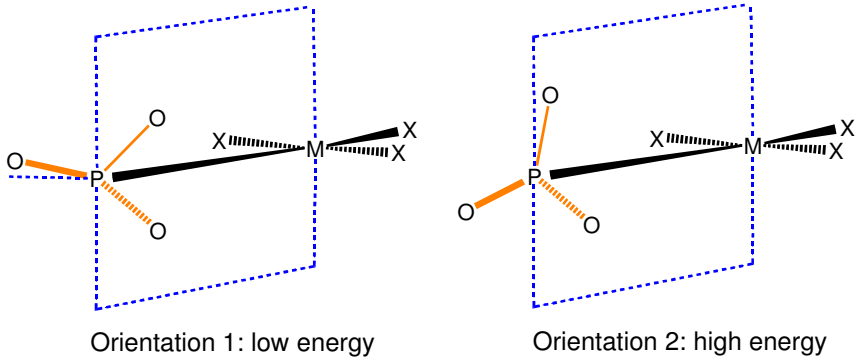

Scheme 2: Orientations of the cyclic ($P(OCH_2)_3CCH_3$) group in square-planar (SQP) [Rh(BID)(CO)($P(OCH_2)_3CCH_3$)] (BID = bidentate ligand with two O donor atoms and charge -1) complexes. The dotted blue quadrilateral indicates a plane perpendicular to the square plane through the complex.

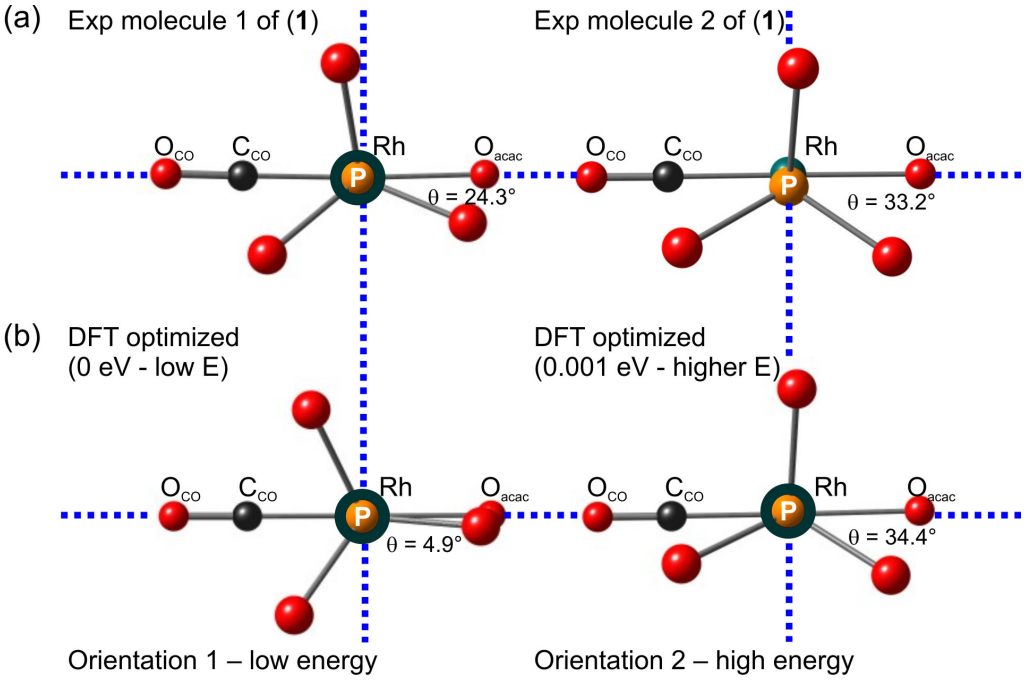

Figure 4: (a) Experimental (two molecules in the asymmetric unit of complex (**1**)) and (b) DFT (PW91/TZP) optimized geometries of complex (**1**), viewed along the P-Rh bond with PO_3 in the front and (OC)Rh(O_{acac}) at the back (selected atoms removed for clarity). θ = dihedral angle O_{acac} *trans* to CO-Rh-P-O. The blue dotted lines show vertical and horizontal planes. Colour code (online version): Rh (green), O (red), P (orange), C (black), O (white).

The energy barrier of rotation of group ($P(OCH_2)_3CCH_3$) in the square-planar complex (**3**), where one phenyl group is attached to the backbone of the cupf-bidentate ligand coordinated to rhodium,

is slightly higher than that of (**1**), namely 0.016 eV, while that of square-planar complex (**2**), with two phenyl groups attached to the backbone of the dbm-bidentate ligand coordinated to rhodium, is slightly more, 0.021 eV. These results indicate that for the three square planar rhodium complexes (**1**) – (**3**) (as the size of the bidentate ligand increases from acac [complex (**1**)] to cupf [complex (**2**)] to dbm [complex (**3**)]), the energy barrier of rotation also increases. However, for the square pyramidal complex (**4**), with a fifth ligand attached to rhodium, the energy barrier of rotation is much larger, namely 0.138 eV. This high energy barrier occurs when a P-O bond is aligned parallel to and on the same side as the Rh-C_{acyl} bond, leading to repulsion between the two oxygens. The lowest energy conformation of complex (**4**) is thus indeed when the distance between the O_{acyl} and any of the oxygens on ($P(OCH_2)_3CCH_3$) is as large as possible; see **Figure 5**. The cyclic ($P(OCH_2)_3CCH_3$) group thus adopts orientation 2 (**Scheme 2**) in both the DFT lowest energy optimized geometry, as well as in the experimental crystal structure of the square pyramidal complex (**4**). The experimental three dihedral angles $O_{cupf\ \textit{trans}\ to\ I}$-Rh-P-O of 34.7°, 81.5° and 153.8° [27], are thus near perpendicular to the plane through the four atoms coordinated to Rh. These dihedral angles should be 45°, 90° and 135°, respectively, to be exactly perpendicular.

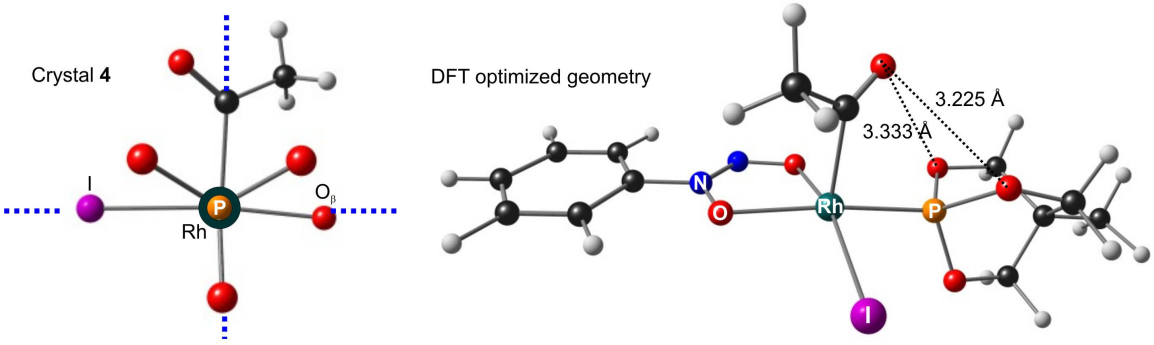

Figure 5: Orientations of the ($P(OCH_2)_3CCH_3$) group in the crystal structure of complex (**4**) [27] and the PW91/TZP optimized geometry of (**4**). Colour code (online version): Rh (green), O (red), N (blue), I (purple), P (orange), C (black), O (white).

In contrast, the orientation of the ($P(OCH_2)_3CCH_3$) group in both the DFT optimized geometry of complex (**2**), as well as in the crystal structure of (**2**), is orientation 1 (**Scheme 2**): where one P-O bond is aligned near parallel to the Rh-$O_{dbm\ \textit{trans}\ to\ CO}$ (dihedral angle $O_{dbm\ trans\ to\ CO}$-Rh-P-O = -6.8° calculated and -10.7° experimental) and the other two P-O bonds are orientated such that both dihedral angles C_{CO}-Rh-P-O are as large as possible, namely 53.1° and -67.2° (experimental) [25], and 52.5° and -66.6° (calculated), see **Figure 6**.

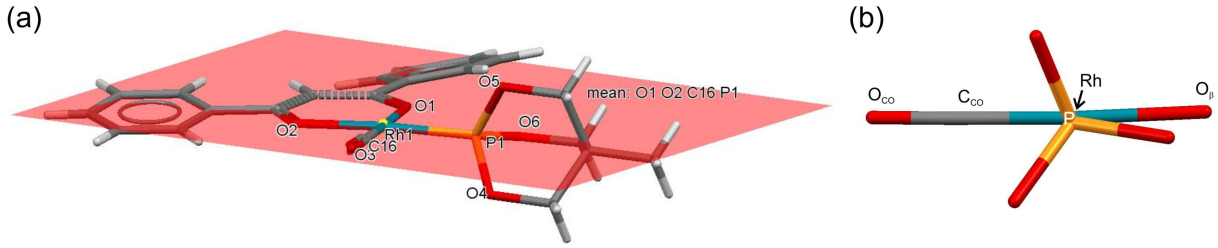

Figure 6: Different views of the experimental crystal geometry of complex (**2**) [25]. (a) The mean plane through $O_{dbm}O_{dbm}C_{CO}P$ shows the orientation of the cyclic ($P(OCH_2)_3CCH_3$) group in the crystal structure of complex (**2**)**.** (b) View along the P-Rh bond with PO_3 in the front and (OC)Rh(O_{dbm}) at the back (selected atoms removed for clarity). Colour code (online version): Rh (blue-green), O (red), P (orange), C (black), O (white).

The DFT calculated minimum energy orientation of the ($P(OCH_2)_3CCH_3$) group in complex (**3**), is also when one of the P-O bonds is aligned near parallel to the plane through the four atoms coordinated to Rh, namely orientation 1 in **Scheme 2**. As stated earlier, in complex (**1**) this P-O bond is orientated on the same side as the Rh-$O_{acac\ trans\ to\ CO}$ bond, as shown in **Figure 7** (a) (i). The alternative DFT optimized geometry, where one P-O bond is aligned near parallel to the Rh-C_{CO} bond, is only 0.0008 eV higher in energy for complex (**1**). For complex (**3**), the DFT optimized geometry with the lowest energy is similar to complex (**1**), namely the geometry where one P-O bond is aligned near parallel to the Rh-$O_{cupf\ trans\ to\ CO}$ bond (**Figure 7** (b) (i)) with dihedral angle $O_{cupf\ trans\ to\ CO}$-Rh-P-O = -0.4°. The alternative DFT optimized geometry with the P-O bond aligned near parallel to the Rh-C_{CO} bond (**Figure 7** (b) (ii)), is 0.0114 eV higher in energy, although the intra molecular distance between $O_{phosphite}$ and C_{CO} is similar to that of complex (**1**) (compare **Figure 7** (b) (ii) with **Figure 7** (a) (ii)). An energy difference of 0.01 eV is not too high for the molecule to exist experimentally. In this case, the orientation of the cyclic $P(OCH_2)_3CCH_3$) group in the experimental structure of complex (**3**), is indeed the slightly higher energy orientation with dihedral angle C_{CO}-Rh-P-O = -2.5° experimental [26] (4.2° calculated), as shown in **Figure 7** (b) (ii).

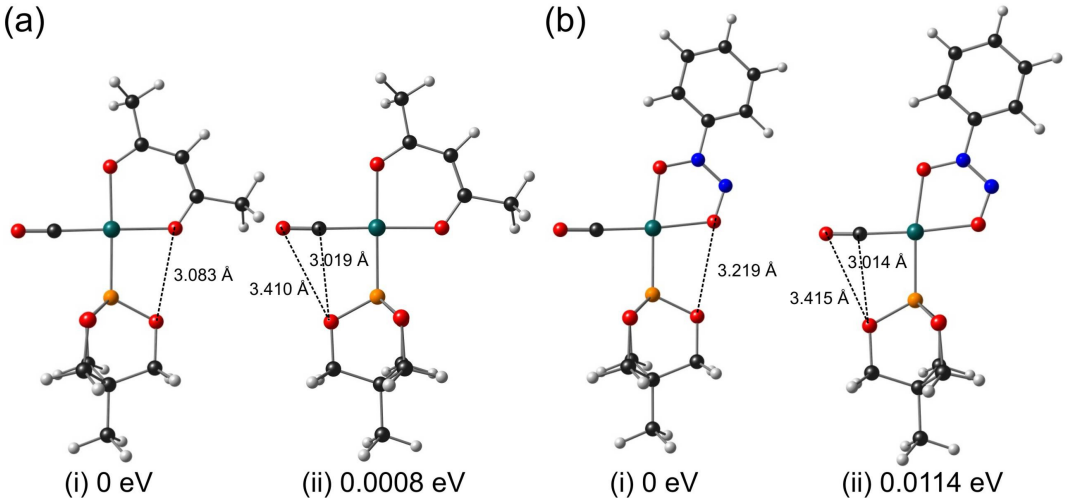

Figure 7: (a) PW91/TZP optimized geometry of (a) complex (**1**) and (b) complex (**3**), optimized with (i) one of the P-O bonds near parallel to the Rh-$O_{BID\ trans\ to\ CO}$ and (ii) with one P-O bond near parallel to CO. Both orientations are as illustrated by orientation 1 in **Scheme 2**. Colour code (online version): Rh (green), O (red), N (blue), P (orange), C (black), O (white).

4 Conclusions

The DFT calculated minimum energy orientation of the cyclic ($P(OCH_2)_3CCH_3$) group in square planar [Rh(BID)(CO)($P(OCH_2)_3CCH_3$)] (BID = bidentate ligand with two O donor atoms and charge -1) complexes containing a bidentate ligand, is with one of the P-O bonds aligned near parallel to the plane through the four atoms coordinated to Rh. The three P-O bonds of the rigid ($P(OCH_2)_3CCH_3$) group, adopt a C_3-symmetrical conformation around the Rh-P axis. The geometry with the lowest energy is where one P-O bond is aligned near parallel to the Rh-$O_{BID\ trans\ to\ CO}$ bond with a dihedral angle $O_{BID\ trans\ to\ CO}$-Rh-P-O < 10°. The geometry with a P-O bond orientated near parallel to the Rh-C_{CO} bond, is slightly higher in energy, but still possible experimentally. The orientation of the ($P(OCH_2)_3CCH_3$) group in available experimental structures of square planar [Rh(BID)(CO)($P(OCH_2)_3CCH_3$)] complexes, confirms this finding.

Appendix A Supporting Information

CCDC 1451827 contains the supplementary crystallographic data for (**1**). These data can be obtained free of charge via http://www.ccdc.cam.ac.uk/conts/retrieving.html, or from the Cambridge Crystallographic Data Centre, 12 Union Road, Cambridge CB2 1EZ, UK; fax: (+44)

1223-336-033; or e-mail: deposit@ccdc.cam.ac.uk. Figure S1, selected crystallographic data and the optimized coordinates of the DFT calculations are given in the Supporting Information.

Acknowledgements

This work has received support from the South African National Research Foundation and the Central Research Fund of the University of the Free State, Bloemfontein, South Africa. The High Performance Computing facility of the UFS is acknowledged for computer time.

References

[1] J.F. Roth, The Production of Acetic Acid Rhodium Catalysed Carbonylation of Methanol, Platinum Metals Rev. 19 (1975) 12-14.

[2] Acetic Acid Market Analysis By Application (VAM, Acetic Anhydride, Acetate Esters, PTA) And Segment Forecasts To 2022, Published: July 2015 | ISBN Code: 978-1-68038-077-4, http://www.grandviewresearch.com/industry-analysis/acetic-acid-market, accessed 10/01/2016

[3] Report, Acetic Acid Market & Its Derivatives (Vinyl Acetate Monomer (VAM), Purified Terephthalic Acid (PTA), Acetic Anhydride, & Ester Solvents- Ethyl Acetate & Butyl Acetate) Market By Applications & Geography – Trends & Forecasts to 2018, http://www.marketsandmarkets.com/PressReleases/acetic-acid.asp, accessed 10/01/2016

[4] P.M. Maitlis, A. Haynes, G.J. Sunley, M.J.J. Howard, Methanol carbonylation revisited: thirty years on, Chem. Soc., Dalton Trans. 11 (1996) 2187-2196. DOI: 10.1039/DT9960002187

[5] A. Haynes, P.M. Maitlis, G.E. Morris, G.J. Sunley, H. Adams, P.W. Badger, C.M. Bowers, D.B. Cook, P.I.P. Elliot, T. Ghaffer, H. Green, T.R. Griffin, M. Payne, J.M. Pearson, M.J. Taylor, P.W. Vickers, R. Watt, Promotion of Iridium-Catalyzed Methanol Carbonylation: Mechanistic Studies of the Cativa Process, J. Am. Chem. Soc. 126 (2004) 2847-2861. DOI**:** 10.1021/ja039464y

[6] C.M. Thomas, G. Süss-Fink, Ligand effects in the rhodium-catalyzed carbonylation of methanol, Coord. Chem. Rev. 243 (2003) 125-142. DOI: 10.1016/S0010-8545(03)00051-1

[7] J. Rankin, A.D. Poole, A.C. Benyei, D.J. Cole-Hamilton, A highly efficient catalyst precursor for ethanoic acid production: [$RhCl(CO)(PEt_3)_2$]; X-ray crystal and molecular structure of carbonyldiiodo(methyl)bis(triethylphosphine)rhodium(III), Chem. Commun. 19 (1997) 1835-1836. DOI: 10.1039/A703895J

[8] J. Rankin, A.C. Benyei, A.D. Poole, D.J. Cole-Hamilton, The carbonylation of methanol catalysed by [RhI(CO)(PEt_3)$_2$]; crystal and molecular structure of [$RhMeI_2$(CO)(PEt_3)$_2$], Dalton Trans. (1999) 3771-3782. DOI: 10.1039/A905308E

[9] J. Conradie, G.J. Lamprecht, A. Roodt, J.C. Swarts, Kinetic study of the oxidative addition reaction between methyl iodide and [Rh(Fc$COCHCOCF_3$)(CO)(PPh_3)]: Structure of [Rh(Fc$COCHCOCF_3$)(CO)(PPh_3)(CH_3)(I)], Polyhedron 23 (2007) 5075-5087. DOI: 10.1016/j.poly.2007.07.004

[10] M.M. Conradie, J. Conradie, Methyl Iodide Oxidative Addition to Monocarbonylphosphine [Rh((C_4H_3S)COCHCOR)(CO)(PPh_3)] Complexes Utilizing UV/vis and IR Spectrophotometry and NMR Spectroscopy to Identify Reaction Intermediates. R = C_6H_5 or C_4H_3S, Inorg. Chim. Acta. 361 (2008) 2285-2295. DOI: 10.1016/j.ica.2007.10.052

[11] J. Conradie, J.C. Swarts, Oxidative Addition of CH_3I and CO Migratory Insertion in a series of Ferrocene-containing Carbonyl Phosphine β-Diketonato Rhodium(I) Complexes, Organometallics 28 (2009) 1018-1026. DOI: 10.1021/om800655j

[12] N.F. Stuurman, J. Conradie, Iodomethane Oxidative Addition and CO Migratory Insertion in Monocarbonylphosphine Complexes of the type [Rh((C_6H_5)COCHCO((CH_2)$_\eta CH_3$))(CO)(PPh_3)]: Steric and Electronic Effects, J Organomet. Chem. 694 (2009) 259-268. DOI: 10.1016/j.jorganchem.2008.10.040

[13] G.J. Van Zyl, G.J. Lamprecht, J.G. Leipoldt, T.W. Swaddle, Kinetics and mechanism of the oxidative addition of iodomethane to β-diketonatobis(triphenylphosphite)rhodium(I) complexes, Inorg. Chim. Acta 143 (1988) 223-227. DOI: 10.1016/S0020-1693(00)83693-2

[14] M.M. Conradie, J. Conradie, A Density Functional Theory Study of the Oxidative Addition of Methyl Iodide to Square Planar [Rh(acac)($P(OPh)_3$)$_2$] complex and simplified model systems, J. Organomet. Chem. 695 (2010) 2126-2133. DOI: 10.1016/j.jorganchem.2010.05.021

[15] M.M. Conradie, J.J.C. Erasmus, J. Conradie, Iodomethane oxidative addition to β-Diketonatobis(triphenylphosphite)rhodium(I) complexes: A synthetic, kinetic and computational study, Polyhedron 30 (2011) 2345-2353. DOI: 10.1016/j.poly.2011.06.017

[16] J.J.C. Erasmus, J. Conradie, Chemical and electrochemical oxidation of [Rh(β-diketonato)(CO)($P(OCH_2)_3CCH_3$)]: an experimental and DFT study, Dalton Trans. 42 (2013) 8655–8666. DOI:10.1039/C3DT50310K

[17] J.J.C. Erasmus, J. Conradie, Oxidative Addition of Methyl Iodide to [Rh(PhCOCHCOPh)(CO)($P(OCH_2)_3CCH_3$)]: an experimental and computational study, Cent. Eur. J. Chem. 10 (2012) 256-566. DOI: 10.2478/s11532-011-0137-0

[18] J.J.C. Erasmus, M.M. Conradie, J. Conradie, Kinetics and Mechanism of the Oxidative Addition of Methyl Iodide to [Rh($CH_3COCHCOCF_3$)(CO)($P(OCH_2)_3CCH_3$)]: an experimental and computational study, Reac. Kinet. Cat. Lett. 105 (2012) 233-249. DOI: 10.1007/s11144-011-0413-1

[19] J.J.C. Erasmus, J. Conradie, Oxidative Addition of Methyl Iodide to [Rh($CH_3COCHCOCH_3$)(CO)($P(OCH_2)_3CCH_3$)], Inorg. Chim. Acta 375 (2011) 128-134. DOI: 10.1016/j.ica.2011.04.041

[20] V. Bocokić, A. Kalkan, M. Lutz, A. L. Spek, D.T. Gryko, J.N.H. Reek, Capsule-controlled selectivity of a rhodium hydroformylation catalyst, Nature Communications, 4:2670 (2013) 1-9. DOI: 10.1038/ncomms3670

[21] J. Conradie, Conformational analysis of triphenylphosphine in square planar organometallic complexes: [(PPh_3)($ML_1L_2L_3$)] and [M(acac)(L′)(PPh_3)], Dalton Trans. 41 (2012) 10633-10642. DOI:10.1039/C2DT30850A.

[22] N.F. Stuurman, A. Muller, J. Conradie, Conformational analysis of triphenylphosphine in square planar [Rh(β-diketonato)(CO)(PPh_3)] complexes. Crystal structure of [Rh(PhCOCHCO($CH_2)_3CH_3$)(CO)(PPh_3)], Inorg. Chim. Acta, 295 (2013) 237–244 DOI: 10.1016/ j.ica.2012.11.001

[23] N.F. Stuurman, A. Muller, J. Conradie, Structural trends in [Rh(PhCOCHCO($CH_2)_nCH_3$)(CO)(PPh_3)] (n = 0 – 3) and related complexes. Crystal structure of [Rh(PhCOCHCO($CH_2)_2CH_3$)(CO)(PPh_3)], Trans. Met. Chem. 38 (2013) 429–440. DOI: 10.1007/s11243-013-9708-6

[24] W. Purcell, J. Conradie, T.T. Chiweshe, J.A. Venter, H.G. Visser, M.P. Coetzee, Characterisation of acetylacetonato carbonyl diphenyl-2-pyridylphoshine rhodium(I): Comparison with other carbonyl complexes, J. Mol. Struct. 1038 (2013) 220–229 DOI: 10.1016/j.molstruc.2013.01.061.

[25] J.J.C. Erasmus, G.J. Lamprecht, T. Kohzuma, Y. Nakano, Carbonyl(1,3-diphenyl-l,3-propanedionato-O,O') (4-methyl-2,6,7-trioxa- 1-phosphabicyclo[2.2.2]octane-P)rhodium(I), Acta Cryst. C54 (1998) 1085-1087. DOI: 10.1107/S0108270198002388

[26] S.S. Basson, J.G. Leipoldt, W. Purcell, J.A. Venter, Structure of carbonyl(N-hy-droxy-N-nitrosobenzenaminato-O,O')(4-methyl-2,6,7-trioxa-1-phosphabi-cyclo[2.2.2]octane)rhodium(I), Acta Cryst. C48 (1992) 171-173. DOI: 10.1107/S0108270191008223

[27] J.A. Venter, W. Purcell, H.G. Visser, Di-l-iodido-bis[acetyl(4-methyl-2,6,7-trioxa-1-phosphabicyclo[2.2.2]octane)-(N-nitroso-N-oxidoaniline-j2O,O0)-rhodium(III)], Acta Cryst. E65 (2009) m1528-m1529. DOI: 10.1107/S1600536809043050

[28] F. Bonati, G. Wilkinson, Dicarbonyl-β-diketonato- and related complexes of rhodium(I), J. Chem. Soc. 39 (1964) 3156-3160. DOI: 10.1039/JR9640003156

[29] C.W. Heitsch, J.G. Verkade, Phosphorus Complexes of Group III Acids. I. Boron Acids and 4-Methyl-2,6,7-trioxa-l-phosphabicyclo[2.2.2]octane, Inorg. Chem. 1 (1962) 392-398. DOI: 10.1021/ic50002a039

[30] APEX2 (including SAINT and SADABS); Bruker AXS Inc., Madison, WI, 2012.

[31] G.M. Sheldrick, A short history of SHELX, Acta Cryst. A 64 (2008) 112-122. DOI: 10.1107/S0108767307043930

[32] G. te Velde, F.M Bickelhaupt, E.J. Baerends, C. Fonseca Guerra, S.J.A. van Gisbergen, J.G. Snijders, T. Ziegler, Chemistry with ADF, J. Comput. Chem. 22 (2001) 931-967. DOI: 10.1002/jcc.1056

[33] J.P. Perdew, J.A. Chevary, S.H. Vosko, K.A. Jackson, M.R. Pederson, D.J. Singh, C. Fiolhais, Atoms, molecules, solids, and surfaces: Applications of the generalized gradient approximation for exchange and correlation, Phys. Rev. B 46 (1992) 6671-6687. Erratum: J.P. Perdew, J.A. Chevary, S.H. Vosko, K.A. Jackson, M.R. Perderson, D.J. Singh, C. Fiolhais, Phys. Rev. B 48 (1993) 4978. DOI: http://dx.doi.org/10.1103/PhysRevB.46.6671

[34] L.J. Farrugia, WinGX and ORTEP for Windows: an update, J. Appl. Crystallogr. 45 (2012) 849-854. DOI:10.1107/S0021889812029111